Isolation and Physicochemical Characterization of the Half-Unit Membranes of Oilseed Lipid Bodies

T.J. Jacks*[a], T.P. Hensarling[a], J.N. Neucere[a], L.Y. Yatsu[a] and R.H. Barker[b]
[a]Southern Regional Research Center, P.O. Box 19687, New Orleans, LA 70179; and [b]American Fiber Manufacturers Association, Washington, DC 20036

The lipid-free residue of lipid body membranes was isolated from quiescent peanuts and was physicochemically characterized. The preponderant component of the residue was proteinaceous and consisted of at least two polypeptides according to ultracentrifugation, gel filtration, gel electrophoresis and HPLC. The molecular weight of the principal polypeptide was between 10,000 and 16,000 daltons. Only one antigen, immunochemically unique with respect to other peanut components, was detected. Spectral analyses indicated the presence of a protoheme and revealed conformational modes of β-sheet and unordered structure but no α-helix. The amino acid composition was similar to that of an integral membrane polypeptide rather than to those of peripheral membranes or other plant polypeptides. The hydrophobicity, conformation and quantitative content of polypeptides were suitable for the existence of a monolayer at the lipid body-cytoplasm interface. The results indicated that lipid body coatings physicochemically resemble membranes of intracellular organelles and supported the morphological concept that the coatings are half-unit biological membranes. Reutilization of lipid body membranes appeared possible after lipid depletion during seed germination.

Lipid bodies (spherosomes, oleosomes) are intracellular particles about 1–2 μm in diameter that are the principal repository sites of lipid reserves in oilseeds (1,2). The lack of morphologically discernible tripartite-structured membranes surrounding lipid bodies had been perplexing until the concept of half-unit membranes to describe the coatings was proposed (3). Subsequently, the concept has been used on a morphological basis (1,2). To determine whether the coatings are also similar biochemically to membranes of cellular organelles, we conducted large-scale isolation and physicochemical characterizations of the lipid-free residue of peanut lipid body membranes.

EXPERIMENTAL PROCEDURES

Tissue. Shelled peanut seeds (*Arachis hypogaea* L.), Virginia 56R variety, were freed of testae and stored at 5°C. At dryness, seeds were 29% protein and 48% lipid by weight.

Electron microscopy. The isolation of lipid bodies was monitored with electron microscopy. To facilitate the manipulation of isolated lipid bodies through preparative procedures, specimens were mixed with 2% (w/v) agar at 43°C and centrifuged at 2,600 *g* until the agar gelled. Portions of lipid body-enriched gel and pieces of whole cotyledonary tissue (approximately 0.3 mm^3) were prepared for sectioning as described previously (4). Thin sections of epoxy-embedded specimens were cut on a Servall MT-1 Porter-Blum ultramicrotome with a diamond knife and were examined with either a Philips EM 200 or EM 300 electron microscope.

TABLE 1

Components of Defatted Lipid Body Membrane

Component	Content (% w/w)
RNA	0.6
Hexosamine	1.1
Neutral hexose	0.3
Sialic acid	0.0[a]
Nitrogen	11.0
Phosphorus	0.6
Sulfur	0.5
Iron	0.2

[a]Not detected in 10 mg of sample.

Chemical analyses. Nitrogen and phosphorus were assayed colorimetrically (5,6). In addition, nitrogen and phosphorus as well as iron and sulfur were determined by electron emission spectra (ESCA) using a Varian IEE 15 spectrometer as described by Soignet *et al.* (7). Phospholipid content was determined by 24.8 × lipid phosphorus.

Hexose and hexosamine were determined colorimetrically (8). Hexose was assayed after sample hydrolysis (9) and hexosamine was measured as hexose after hydrolysis and deamination (10) with corrections for hexose content before deamination; deaminating reagents did not interfere with hexose estimation. Sialic acid also was assayed colorimetrically (11).

Total lipid content was measured gravimetrically after extraction from dried samples as described earlier (4).

Protein was determined by the method of Lowry *et al.* (12). Amino acid analyses were conducted by Worthington Biochemical Corporation, Freehold, New Jersey. The amino acid composition of the defatted lipid body residue indicated an average content of 10.6% nitrogen by weight for a nitrogen-to-protein conversion factor of 9.4.

Nucleic acids were isolated by a modified procedure of Caldwell and Henderson (13). In brief, dried samples were homogenized (1 mg/mL) in 5.0 mM phosphate buffer (pH 7.9) containing 0.5 M NaCl and 0.25% sodium deoxycholate, and centrifuged. Nucleic acids in supernatants were detected spectrofluorometrically as ethidium bromide complexes (14); loss of fluorescence after RNAase treatment (at 50°C for 1 hr) corresponded to RNA, and residual fluorescence was assigned to DNA.

Enzyme analyses. Acid proteinase, acid phosphatase and glucose-6-phosphatase activities were determined

*To whom correspondence should be addressed.

TABLE 2

Amino acid composition of lipid body protein

Amino acid	Mole %
Lys	3.9
His	1.4
Arg	4.4
Asp	6.2
Thr	9.2
Ser	7.9
Glu	6.5
Pro	4.6
Gly	13.9
Ala	11.9
Val	6.2
Met	1.4
Ile	4.6
Leu	9.7
Tyr	4.4
Phe	3.5
Cys	0.3
Trp	trace

by measuring the rates of hydrolysis of hemoglobin (15), phenyl phosphate (16) and glucose-6-phosphate (17), respectively. Catalase activity was estimated by measuring the disappearance of hydrogen peroxide, which was assayed as peroxytitanium sulfate (18). Isocitrate lyase activity was determined by continuously measuring the production of glyoxylate, which was assayed as the phenylhydrazone (19), from L_s-isocitrate. NAD-isocitrate dehydrogenase and alcohol dehydrogenase activities were estimated by continuously measuring the rates of reduction of NAD (20,21) in the presence of L_s-isocitrate and ethanol, respectively. Lipase activity was estimated by determining the production of fatty acids from emulsified triglycerides (4), and by measuring the fluorescence produced by hydrolysis of 4-methylumbelliferone from its heptanoyl derivative (22).

The rate of the reaction catalyzed by each enzyme was linear, and proportionality was observed between each rate and amount of enzyme when enzyme was rate limiting.

Spectral analyses—visible, ultraviolet, infrared and circular dichroic. For visible and ultraviolet spectra, specimens were dissolved in either 0.05 M Tris-HCl (pH 8.0) containing 1% (w/v) Triton X-100 (23) or in ethanol/acetonitrile/water (EAW, 4:1:1, v/v/v), respectively. EAW did not absorb a significant amount of ultraviolet irradiation and readily dissolved the lipid-free residue of lipid bodies. Triton X-100 solvents absorbed significant amounts of ultraviolet light; therefore, spectrophotometric measurements in the presence of Triton X-100 were confined to visible wavelengths. In certain instances, specimens were reduced with a few grains of sodium dithionite and oxidized with H_2O_2 or ammonium persulfate. All visible and ultraviolet spectra were obtained with a Beckman Model DK-2A ratio-recording spectrophotometer.

Infrared spectra of specimens in KBr discs and Nujol mulls were recorded with a Perkin-Elmer Model 621 spectrophotometer.

Circular dichroic spectra of specimens dissolved in EAW were obtained with a Cary Model 60 spectropolarimeter equipped with 6001 CD optics. Amounts of α-helical, β-sheet and unordered conformational modes were calculated by comparing ellipticity values for each specimen with values for conformationally known polypeptides at several wavelengths as determined and described by Greenfield and Fasman (24). A mean residue weight of 158.5 g mole^{-1} was calculated from amino acid data.

Analytical ultracentrifugation. Specimens dissolved in 0.05 M Tris-HCl (pH 8.0) containing 1% (w/v) Triton X-100 were centrifuged at 59,780 RPM in synthetic boundary cells of the Spinco model E ultracentrifuge equipped with schlieren optics. Fringe displacements were assessed with a Nippon Kogaku 2-dimensional microcomparator. Molecular weights were derived by the method of Halsall (25) from sedimentation values calculated according to Schachman (26). The value of 0.736 cm^3 g^{-1} for the partial specific volume of the specimen was calculated from the amino acid content.

Gel electrophoresis. SDS-PAGE and Triton X-100-PAGE were performed according to Laemmli (27) and Singh and Wasserman (23), respectively.

Gel filtration and HPLC. Gel filtration on Sephadex LH-20 was conducted by the method of Shannon and Hill (28) except that the solvent was either EAW or EAW adjusted to pH 8.5 with NH_4OH.

HPLC was performed with a Waters Associates system equipped with their I-60 protein column using EAW as a solvent.

Immunochemistry. Immunodiffusion and immunoelectrophoresis were performed on defatted residues of lipid bodies and on peanut proteins according to Ouchterlony (29) and Grabar and Williams (30), respectively, with modifications described by Bjerrum (31). Specimens were dissolved in 0.05 M Tris-HCl (pH 8.0) containing 1% (w/v) Triton X-100, and were applied to 1.5% (w/v) Ionagar gels in 0.025 M veronal buffer (pH 8.2). Peanut proteins and antisera were prepared as described earlier (32, 33).

RESULTS

Isolation of lipid bodies. Lipid bodies are the most abundant particles in oilseed cells and, along with protein-storing aleurone grains (protein bodies), comprise the bulk of the intracellular cytoplasm of cotyledonary cells of quiescent oilseeds (1,2). Earlier studies of peanut lipid bodies (3,4,34) found that isolation from homogenized tissue by bucket centrifugation with washes by hand homogenization was inadequate for obtaining sufficient quantities of lipid body coatings for thorough biochemical analyses. Instead, the following method was devised and found satisfactory for the routine isolation of large amounts of lipid bodies.

Four kg of dry, testa-free and axis-free peanuts was soaked overnight in distilled water at 4°C, and ground batch-wise in a large Waring Blendor for 1 min with fresh, ice-cold distilled water using 6 volumes of water per g of tissue. The homogenate was filtered through 8 layers of cheesecloth and centrifuged with an air-driven Sharples continuous-flow centrifuge at 18,750 RPM with a flow rate of 2 L/min. The effluent

was then centrifuged with the Sharples at 30,000 RPM with a flow rate of 290 mL/min. This effluent was centrifuged through a continuous-flow DeLaval Gyro Test Unit Separator (laboratory-scale cream separator), which has an upper overflow-exit port for material less dense than the medium and an underflow-exit port for everything else, at a flow rate of about 750 mL/min (measured at the exit port for underflow). The lipid body fraction was obtained from the overflow-exit port in about 2.5 L. The fraction was washed 14 times by suspension and centrifugation with the DeLaval with the following solutions: 3 times in distilled water, 5 times in 0.5 M NaCl containing 0.05 M Tris-HCl (pH 7.2), once in 0.2 M NaCl containing 0.02 M Tris-HCl (pH 7.2), 5 times in distilled water. Each time the volume of the wash medium was 10 L. The buffered salt solution was used to remove globulins, the most abundant protein component of oilseeds (35). Electron microscopic examination of the final DeLaval overflow showed that only lipid bodies were present, and that their structural integrity was maintained after isolation without coalescence (Fig. 1). Figure 2 shows schematically the isolation procedure. The final fraction in about 2.2 L contained 24.9% water by weight and was stored at −20°C. When dried *in vacuo* over P_2O_5, lipid bodies were composed, by weight, of 99.55% lipid and 0.45% nonlipid residue. Phospholipid and protein contents were 0.09% and 0.22%, respectively, by weight.

The purity of the isolated lipid bodies was estimated by assaying the fraction for marker enzymes of subcellular compartments of the cytoplasm. The activities of acid proteinase—protein bodies (36), acid phosphatase—mainly protein bodies, some cytosol (36), glucose-6-phosphatase—microsomes (37), catalase—microbodies (37,38), isocitrate lyase—microbodies (37,38), NAD-isocitrate dehydrogenase—mitochondria (39), and alcohol dehydrogenase—cytosol (36) were not detected in the lipid body fraction, indicating the absence of contamination of the isolated lipid bodies by these cytoplasmic components. Lipase activity was not detected in the lipid body fraction, as noted previously (4).

Isolation of the defatted residue of lipid body membranes. Since isolated lipid bodies are devoid of any internal organization or structure—shown in Figure 1, top and bottom, and reviewed (1,2)—removal of the lipid from isolated lipid bodies produces only defatted residues of lipid body membranes. Indeed, electron microscopic examinations of lipid bodies exposed to lipid solvents *in situ* and *in vitro* showed that only lipid body coatings remain after lipid removal (3,4,40). Therefore, the following procedure was devised for isolating the defatted residues of lipid body membranes using appropriate solvents to dehydrate specimens and to thoroughly extract both polar and nonpolar lipids (6). Eight hundred mL of the lipid body fraction was added to 8 L of acetone at −20°C. The mixture was continually stirred until it reached about −10°C. Then, 3 L of hexane at room temperature was added and the monophasic mixture was stirred occasionally for 30 min. It was then packed in ice and set aside for 1 hr. The supernatant was carefully decanted and the residue was collected by vacuum filtration. The residue was washed once by suspension in 2 L of ice-cold hexane/acetone (3:2, v/v) and collected by filtering, and twice in 1 L of ice-cold acetone. The acetone-washed residue was then suspended in about 100 mL of ice-cold ether and centrifuged at 8,000 *g* for 10 min. The residue was washed twice with ether. The final precipitate was suspended in a small amount of ether and stored at −20°C. Figure 3 shows schematically the procedure used to isolate the lipid-free residue from lipid bodies. The material was grey-brown and fluffy in ether, and became vitreous when dried. Electron microscopic examinations of the product at widely ranging magnifications revealed no discernible gross or fine organization.

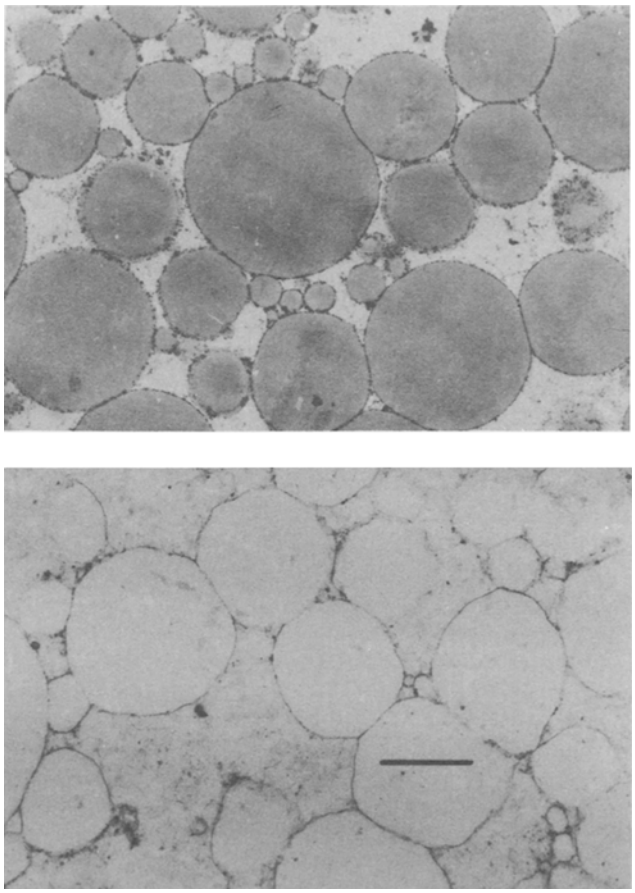

FIG. 1. Electron micrographs of isolated lipid bodies: top, lipid bodies in agar fixed in OsO_4; bottom, lipid bodies in agar fixed in OsO_4 after treatment with hexane. Bar represents 1 μm and suffices for both micrographs.

Components of the defatted residue of lipid body membranes. The composition of the defatted lipid body residue was determined (Table 1). Residual fluorescence from nucleic acid-bound ethidium bromide was absent after RNAase treatment, and was unaffected by DNAase. Thus, all of the nucleic acid, 0.6% by weight, was assigned to RNA. Phosphorus in this amount of RNA would comprise less than 0.1% phosphorus, by weight, indicating something other than nucleic acid contributed to the total phosphorus con-

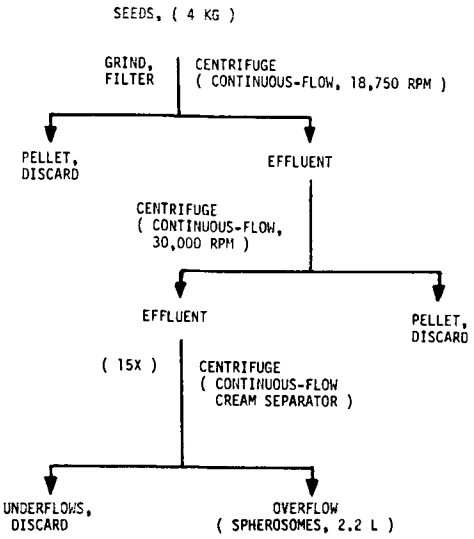

FIG. 2. Flow diagram showing isolation of lipid bodies.

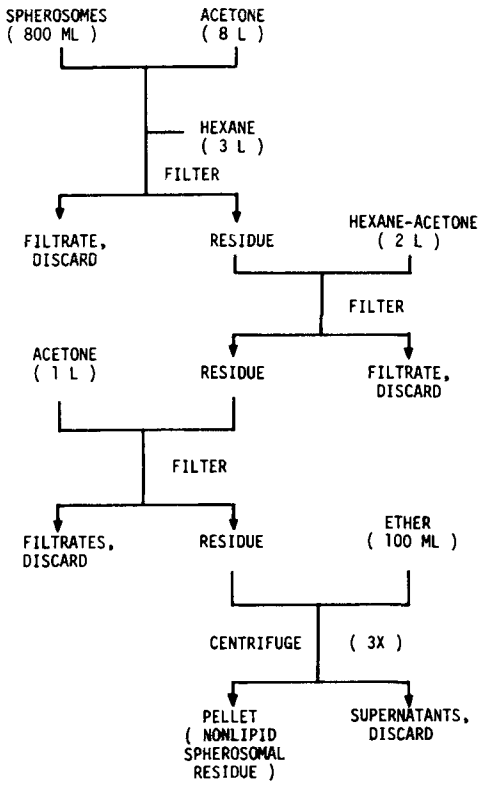

FIG. 3. Flow diagram showing preparation of nonlipid residue of isolated lipid bodies.

tent of 0.6% by weight (Table 1). Since the lipid body residue was lipid-free, phosphorus from phospholipid was absent.

The content of carbohydrate (Table 1) in the lipid body coating was at least tenfold lower than that in membrane preparations (28,41), possibly because of the removal of glycolipids during the defatting process. Alternatively, the nonlipid residue contained low levels of glycoproteins. Sialic acid was not detected in the preparation and has not been reported to be present in plant membranes.

Nitrogen comprised the most abundant component of the defatted residue (Table 1). From the amount of amide nitrogen and the amino acid composition (Table 2), the polypeptide content of the defatted membranes of lipid bodies was estimated at 101% by weight.

The content of cysteine (Table 2) accounted for only 10% of the sulfur in the preparation (Table 1). About 26% of the total sulfur was disulfide and 74% was reduced thiol, according to ESCA. The protoheme associated with lipid bodies—Figure 4 and (42)—contributed to the content of 0.2% iron (Table 2).

Amino acid composition of lipid body membrane-associated polypeptide (MAP). The amino acid composition of MAP was determined for comparison to other plant proteins (Table 2). Compositions were compared using the deviation function (D) of Harris *et al.* (43): $D = [\Sigma(X_{1,i} - X_{2,i})^2]^{1/2}$, where $X_{1,i}$ represents the mole fraction of amino acid i in protein 1, and $X_{2,i}$ represents the mole fraction of the same amino acid in protein 2. D values comparing MAP to other polypeptides and proteins, calculated from data of Table 1 and appropriate references (33, 44-56), are given in Table 3. In addition, the average hydrophobicity per residue ($H\theta_{av}$) (57), calculated from the amino acid composition in Table 2, was 1.055 cal/residue for MAP, a value similar to those obtained of integral membrane proteins (Table 3).

Using amino acid compositions and hydrophobicity values of proteins and polypeptides listed in Table 3, we calculated the discriminant functions, Z, of Barrantes (58): $Z = -0.345$ [(mole fractions of Lys + Arg + His + Asx + Glx)/(mole fractions of Ile + Tyr + Phe + Leu + Val + Met)] + 0.6 $H\theta_{av}$. This function maximizes the discrimination between integral membrane components ($Z = 0.52 +/-0.11$), and peripheral membrane components ($Z = 0.12 +/-0.16$). The value of Z for MAP, 0.37 (Table 3), indicates that MAP is an integral membrane component.

Visible and ultraviolet spectra of MAP. The visible spectrum of MAP indicated the presence of a protoheme (Fig. 4). An absorbance maximum at 410 nm occurred in the oxidized-minus-reduced spectrum (Fig. 4), which was noted previously (42). The ultraviolet spectrum (Fig. 5) revealed two maxima near 280 and 230 nm due to the presence of aromatic amino acids.

Infrared and circular dichroic spectra of MAP. To estimate conformational modes in MAP, infrared and circular dichroism spectra were obtained. In the infrared spectrum (Fig. 6), the main peaks of the amide I and II bands were located at about 1650 cm^{-1} and 1520 cm^{-1}, respectively. Two peaks, one on each side of 1525 cm^{-1}, more clearly comprised the amide II band when the sample was prepared in a Nujol mull. The amide V band occurred at 690 to 700 cm^{-1}. Amide I, II and V bands at these frequencies indicate the

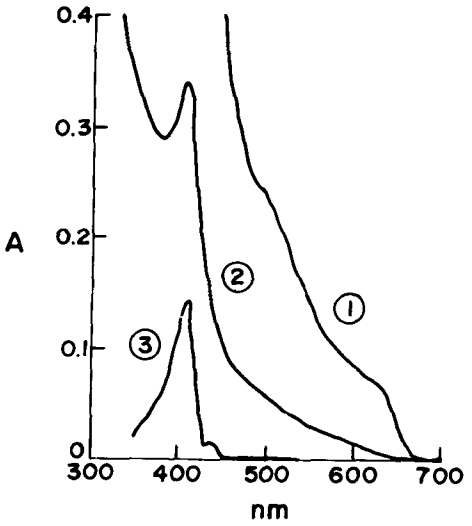

FIG. 4. Visible spectra of MAP: 1, spectrum of specimen in buffered detergent; 2, spectrum of previous solution diluted 5.3-fold; 3, oxidized minus reduced spectrum of second solution.

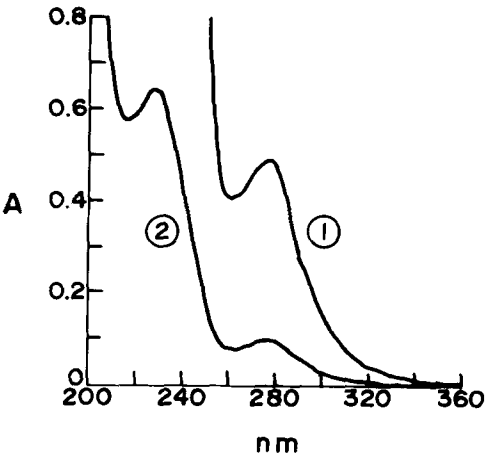

FIG. 5. Ultraviolet spectrum of MAP in EAW: 1, 0.44 mg mL^{-1}; 2, previous solution diluted five-fold.

TABLE 3

Comparison of Polypeptides of Peanut Lipid Bodies to Membrane and Nonmembrane Proteins and Polypeptides of Plants

Source	D[a]	$H\theta_{av}$[b]	Z[c]	Class[d]
Peanut lipid bodies		1.055	0.37	int
Maize lipid bodies ORF-1[e]	0.089	1.018	0.36	int
Yeast mitochondria[f]	0.094	1.156	0.38	int
Spinach chloroplast lamellae[g]	0.083	1.194	0.43	int
Archaebacterial spheroplasts[h]	0.084	1.193	0.50	int
Spinach chloroplasts[i]	0.084	1.151	0.08	per
Maize lipid bodies[j]	0.075	0.919	0.18	per
Wheat chloroplasts[k]	0.079	1.040	0.23	per
Bean chloroplasts[k]	0.072	1.072	0.29	per
Oilseed albumins[l]	0.179	0.780	−0.22	non
Peanut hemagglutinin[m]	0.176	0.774	0.04	non
Oilseed globulins[n]	0.171	1.002	0.07	non
Mustard cytoplasmic GPDH[o]	0.113	0.986	0.16	non

[a]Deviation function calculated according to Harris *et al.* (43). The higher the value, the more dissimilarity in the amino acid composition to that of peanut lipid body membrane; values over 0.100 represent unrelated polypeptides.
[b]Average hydrophobicity per amino acid residue (kcal/mole) calculated according to Bigelow (57).
[c]Discriminant function of membrane and nonmembrane polypeptides calculated according to Barrantes (58).
[d]Classes of membrane polypeptides, based on Z values (previous column), corresponding to: int, integral membrane component (Z = 0.52 +/− 0.11) and per, peripheral membrane component (Z = 0.12 +/− 0.16) (58). Non, established nonmembrane polypeptides (Z = 0.16 +/− 0.17) are also listed for comparison.
[e]Calculated from Vance and Huang (44).
[f]Calculated from Yang and Criddle (45).
[g]Calculated from Ji *et al.* (46).
[h]Calculated from Sprott *et al.* (47).
[i]Calculated from Henriques and Park (48).
[j]Calculated from Qu *et al.* (49).
[k]Calculated from Mani and Zalik (50).
[l]Calculated from the averaged composition of albumins from 12 oilseeds (including peanut) (51–53).
[m]Calculated from Dechary *et al.* (54).
[n]Calculated from the averaged composition of globulins from 10 oilseeds (including peanut) (33, 51, 52, 55).
[o]Calculated from the composition of cytoplasmic, NAD-specific GPDH (glyceraldehyde-3-phosphate dehydrogenase) (56).

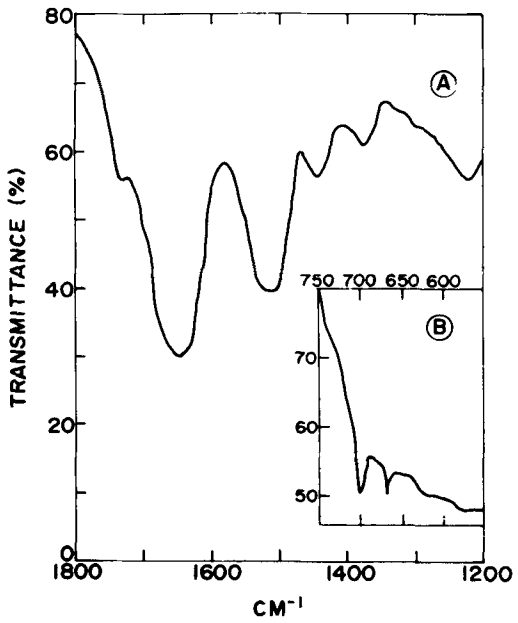

FIG. 6. Infrared spectra of MAP in a KBr disc: A, 1800–1200 cm^{-1}; B, 750–550 cm^{-1}.

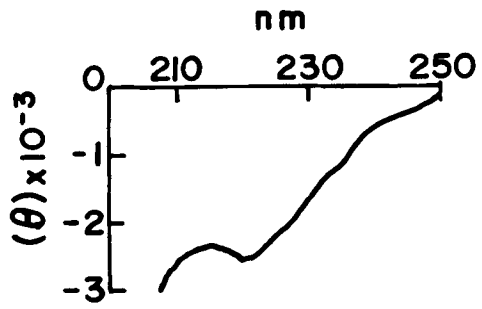

FIG. 7. Far-ultraviolet circular dichroic spectrum of MAP in EAW. Values on the y-axis refer to deg cm^2 $dmol^{-1}$.

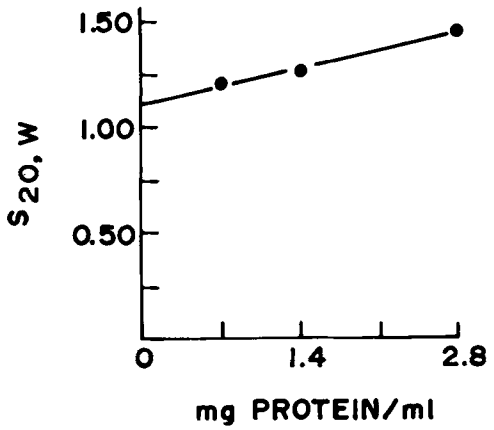

FIG. 8. $S_{20,w}$ of MAP extrapolated to infinite dilution.

preponderant presence of β-sheet and unordered conformational modes (59,60).

A large portion of β-sheet and unordered structure was also detected by circular dichroism (Fig. 7). For these studies MAP was dissolved in EAW. Minimization of differences between our experimental spectrum and spectra of model polypeptides (24) yielded the following conformational modes of MAP: 0.0% α-helical, 30.7% β-sheet and 69.3% unordered structure. The closeness of fit of our experimental spectrum to the theoretical spectrum of a polypeptide with these conformational modes is given by the standard deviation of +/−772 deg cm^2 $dmole^{-1}$. These results indicate that the greater portion of the secondary structure of MAP is unordered with a large planar portion and an absence of helix, indicative of a somewhat flattened and spread-out polypeptide.

Ultracentrifugation of MAP. The standard sedimentation coefficient extrapolated to infinite dilution was 1.1 $S_{20,w}$ (Fig. 8), which corresponded to a molecular weight of 10,000. MAP appeared monodisperse in buffered Triton X-100 during centrifugation but the leading edge of the schlieren peak was skewed, suggesting the presence of an additional component of very closely related size and shape.

Electrophoresis and chromatography of MAP. When MAP was analyzed by SDS-PAGE, the most intensely stained band corresponded to a MW of 16,000 daltons, followed by a component of 33,500 (Fig. 9). When more protein was applied to the gels, bands at 48,000, 86,500 and three more bands between 14,000 and 20,000 daltons appeared. After nondenaturing gel electrophoresis in buffered Triton X-100, only two rather diffuse bands of low molecular weight were apparent (data not shown).

Both filtration of MAP on Sephadex LH-20 in alkaline EAW and HPLC of MAP with a Waters I-60 protein column in EAW revealed two major components (Fig. 10 and 11). The two major peaks in HPLC accounted for 51 and 43%, respectively, of the area under the absorbance curve. Unfortunately, a calibration curve could not be constructed in EAW.

Immunodiffusion and immunoelectrophoresis of MAP. MAP was analyzed immunochemically to determine how many antigenic components comprised MAP and whether previously characterized peanut proteins were possible contaminants of MAP. By immunodiffusion with several concentrations of both antisera and specimens, precipitin reactions between antiserum against MAP with arachin or conarachin—the most abundant peanut proteins (35)—and between antisera against arachin, conarachin or "total cotyledonary extract (32)" (TCE) with MAP were not detected. Antiserum against TCE formed precipitin reactions with TCE but not with MAP. Apparently an antibody against MAP was not in sufficient titer in TCE antiserum to react with MAP. However, antiserum against MAP

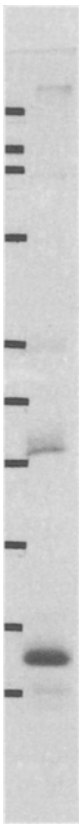

FIG. 9. SDS-PAGE of MAP. The markers on the left of the gel, from top to bottom, correspond to molecular weights ($\times 10^3$) of 205, 116, 97, 66, 45, 36, 29, 24, 20, and 14, respectively.

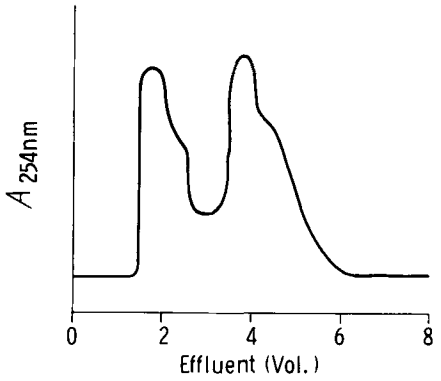

FIG. 10. Gel filtration of MAP in EAW through Sephadex LH-20.

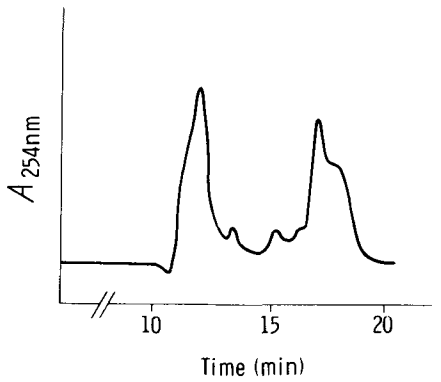

FIG. 11. HPLC of MAP in EAW.

was cross-reactive with TCE; precipitin bands were continuous, indicating identity of the antigen-antibody complex.

Immunoelectrophoretic analysis to determine the number of antigens comprising MAP and whether MAP was contaminated with other peanut polypeptides revealed only one antigenic component in MAP (Fig. 12). MAP and TCE each formed a single precipitin line with MAP antiserum, the latter occurring only with a high titer of antibody. When antiserum against TCE was in the trough, several arcs formed with TCE (Fig. 12), but no reaction occurred with MAP, probably due to low antibody titer.

DISCUSSION

This study addresses the question of whether the limiting boundary of the lipid body-cytoplasm interface in oilseed cells corresponds to a biological membrane. Earlier studies with electron microscopy indicated that the lipid body coating was morphologically an atypical "half-unit" membrane (3). The course taken in this study was to physicochemically characterize the nonlipid portion of the coating, and to determine whether its properties were compatible with the biological membrane concept.

Procedures for large-scale isolation of lipid bodies had to be devised to isolate sufficient amounts since the nonlipid portion comprised less than 0.5% of the dry weight. Large-scale isolation of lipid bodies from homogenized tissue was accomplished by procedures of continuous-flow centrifugation (Fig. 2). Dense particles, e.g. starch grains and proplastids, were removed by the Sharples continuous-flow centrifuge, and particles less dense than the suspending medium were collected with the DeLaval cream separator. Since the bulk of peanut oil consists of oleate residues (61), the density of lipid bodies is estimated at about 0.915 g cm^{-3}, which resulted in their centripetal migration and subsequent concentration above aqueous media during centrifugation.

The purity of the isolated lipid bodies was determined both biochemically and morphologically. Activities of marker enzymes for specific subcellular compartments of the cytoplasm (36–39) were not detected in the lipid body fraction, indicating that the isolated lipid bodies were not contaminated with protein bodies, microsomes, microbodies (including both peroxisomes and glyoxysomes), mitochondria, nor cytosol. Additional evidence for the lack of contamination by protein bodies and cytosol was the absence of proteins associated with those subcellular compartments. Mito-

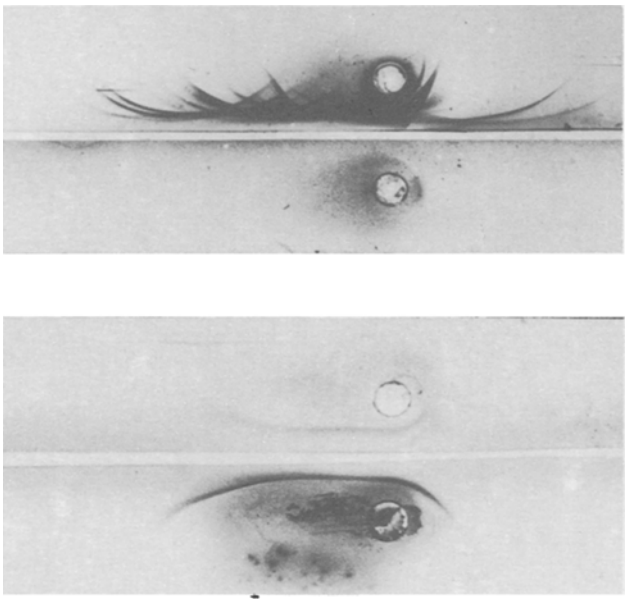

FIG. 12. Immunoelectrophoresis of MAP and total peanut polypeptides: top gel, TCE (upper well) and MAP (lower well) with antiserum against TCE (trough); bottom gel, same except with antiserum against MAP (trough).

chondrial cytochromes were absent and the lack of DNA in the fraction indicated the absence of nuclei.

Morphological evidence for the purity of the isolated lipid bodies was the absence of other cytoplasmic structures in the fraction as determined by examination with electron microscopy. The electron micrographs of Figure 1 are representative of typical fields of view of the lipid body fraction. The electron dense deposits shown as randomly dispersed dots in Figure 1 were artefacts such as osmium-reactive contaminants in the agar embedding medium.

The final preparative procedure (Fig. 3) consisted of a thorough extraction of polar and nonpolar lipids to provide defatted residues of lipid body membranes for subsequent biochemical analyses.

Since the preponderant component of the nonlipid residue from lipid bodies was proteinaceous, understanding the properties of MAP became the major concern to ascertain the membrane character of lipid body coatings. Any other function of this protein is unclear because lipolytic activities (62-64) are remarkably absent in peanut lipid bodies, even when isolated from lipolytically active peanut seedlings (4,34,65).

Results of several methods of comparing the amino acid composition of MAP with compositions of other peanut, plant and membrane polypeptides (Table 3) indicated that MAP more closely resembled integral membrane polypeptides rather than other polypeptides.

The existence of at least two polypeptides comprising MAP was revealed by the skewed schlieren peak during ultracentrifugation in buffered Triton X-100, electrophoresis in buffered Triton X-100, gel filtration on LH-20 (Fig. 10), and HPLC with EAW (Fig. 11).

According to immunochemical analysis, however, MAP contained only one detectable antigen. Either separation and detection of closely related MAP components did not occur during immunodiffusion and immunoelectrophoresis (Fig. 12) or only one MAP component was antigenic. In contrast, six distinct components of MAP were found with SDS-PAGE (Fig. 9), in which proteins are denatured and dissociated into monomeric species. Three of the components, including the most intensely stained band, were smaller than 20,000 MW. Indeed, our molecular weight determinations by ultracentrifugation and SDS-PAGE indicated that the principal MAP polypeptide was within the usual range of molecular weights (10,000-20,000 daltons) reported for the predominant polypeptides of lipid bodies (44,66-68). Experiments to isolate and further characterize one or more of the principal polypeptides comprising MAP are anticipated.

Whether the amount of MAP present per lipid body was quantitatively sufficient and physically suitable to cover the surfaces of lipid bodies was estimated from the following theoretical considerations. A polypeptide at an oil-water interface is fully spread because intermolecular cohesion is lacking due to disruption of van der Waals' forces upon penetration of oil to nonpolar residues (69). This corresponds to a thickness of 0.5 nm. The percentage of the volume of a sphere occupied by a relatively thin surface layer is given by $100 \times 6t/D$, where t is the thickness of the layer and D is the diameter of the sphere. Therefore, for lipid bodies with diameters of 1.0, 1.5, and 2.0 μm, a surface monolayer of polypeptide would represent 0.3, 0.2, and 0.15% of the total volume, respectively. Isolated lipid bodies contained sufficient polypeptide to cover the particulate population of 1.5 μm mean diameter with one layer of polypeptide. A polarity ratio (70) of 1.09, calculated from Table 2, and the discriminant function (Table 3) are consistent with oil-water interfacial localization for MAP but do not preclude other types of interactions. The preponderance of β-sheet and unordered conformational modes determined by infrared and circular dichroic spectra (Fig. 6, 7) is consistent with a polypeptide that would be unconstrained to cover the maximum possible surface area at an oil-water, or lipid body-cytoplasm, interface. However, Vance and Huang (44) proposed a hypothetical model for the principal polypeptide from corn lipid bodies in which a hydrophobic helical portion extends into the lipid body interior, and an amphipathic helical portion lies coiled on the outer surface. Their model, which contains a substantial amount of α-helix, was based on a secondary structure predicted from the amino acid sequence. Experimentally determined secondary structure would be of considerable interest and is needed to substantiate their model.

In addition to serving as a site for storing lipid for respiration and gluconeogenesis in oilseeds, lipid bodies might also serve as precursors for membrane biosynthesis during germination. An extremely rapid proliferation of organelles, particularly endoplasmic reticulum (ER), occurs at the onset of germination (71). New ER contains very low molecular weighted mem-

brane polypeptides (72) and is physically close to lipid bodies (71), which disappear during germination. Perhaps lipid body membranes are transformed to ER upon depletion of the stored lipid in the lipid bodies. Furthermore, the protoheme (Fig. 4) and iron content (Table 1) of lipid bodies might be related developmentally to ER-associated oxidoreductases. Immunological cross-reactivity of MAP from mature peanuts with mitochondrial polypeptide from peanut seedlings (3) implies a conservative transformation of membranes. In contrast, the principal polypeptide of lipid bodies in corn scutella is degraded during germination (66,73). Corn scutella, however, function only during germination; epigeal cotyledons of peanuts and other seeds become photosynthetically functional during seedling growth for which conservation of constituent membrane elements would most likely occur.

ACKNOWLEDGMENTS

J.A. Brockman, D.J. Daigle, E.E. Graves and D.M. Soignet provided valuable technical assistance.

REFERENCES

1. Huang, A.H.C., in *Modern Methods of Plant Analysis,* edited by H.F. Linskens and J.F. Jackson, Springer-Verlag, Berlin, Germany (1985) pp. 145–151.
2. Stymme, S., and A.K. Stobart, in *The Biochemistry of Plants,* edited by P.K. Stumpf and E.E. Conn, Academic Press, Orlando, Florida, (1987), pp. 175–214.
3. Yatsu, L.Y., and T.J. Jacks, *Plant Physiol. 49*:937 (1972).
4. Jacks, T.J., L.Y. Yatsu and A.M. Altschul, *Plant Physiol. 42*:585 (1967).
5. Minari, O., and D.B. Zilversmit, *Anal. Biochem. 6*:320 (1963).
6. Jacks, T.J., L.Y. Yatsu and T.P. Hensarling, *J. Am. Oil Chem. Soc. 47*:222 (1970).
7. Soignet, D.M., R.J. Berni and R.R. Benerito, *J. Appl. Polym. Sci. 20*:2483 (1976).
8. Dubois, M., K.A. Gilles, J.K. Hamilton, P.A. Rebers and F. Smith, *Anal. Chem. 28*:350 (1956).
9. Johansen, P.G., R.D. Marshall and A. Neuberger, *Biochem. J. 77*:239 (1960).
10. Lee, Y.C., and R. Montgomery, *Arch. Biochem. Biophys. 93*:292 (1961).
11. Warren, L., *J. Biol. Chem. 234*:1971 (1959).
12. Lowry, O.H., N.J. Rosebrough, A.L. Farr and R.J. Randall, *J. Biol. Chem. 193*:265 (1951).
13. Caldwell, I.C., and J.F. Henderson, *Anal. Biochem. 34*:303 (1970).
14. LePecq, J.B., and C. Paoletti, *Anal. Biochem. 17*:100 (1966).
15. Anson, M.L., *J. Gen. Physiol. 22*:79 (1938).
16. Salomom, L.L., J. James and P.R. Weaver, *Anal. Chem. 36*:1162 (1964).
17. Nordlie, R.C., and W.A. Arion, *Meth. Enzymol. 9*:619 (1966).
18. Chantrenne, H., *Biochim. Biophys. Acta 16*:410 (1955).
19. Syrett, P.J., and P.C.L. John, *Ibid 151*:295 (1968).
20. Racker. E., *J. Biol. Chem. 184*:313 (1950).
21. Kornberg, A., and W.E. Pricer, *J. Biol. Chem. 189*:123 (1951).
22. Jacks, T.J., and H.W. Kircher, *Anal. Biochem. 21*:279 (1967).
23. Singh, J., and A.R. Wasserman, *Biochim. Biophys. Acta 221*:379 (1970).
24. Greenfield, N., and G.D. Fasman, *Biochemistry 8*:4108 (1969).
25. Halsall, H.B., *Nature 215*:880 (1967).
26. Schachman, H.K., *Meth. Enzymol. 4*:32 (1957).
27. Laemmli, U.K., *Nature 227*:680 (1970).
28. Shannon, C.F., and J.M. Hill, *Biochemistry 10*:3021 (1971).
29. Ouchterlony, O., *Acta Pathol. Microbiol. Scand. 26*:507 (1949).
30. Grabar, P., and C.A. Williams, *Biochim. Biophys. Acta 10:* 193 (1953).
31. Bjerrum, O.J., in *Membrane Proteins: A Laboratory Manual,* edited by A. Azzi, U. Brodbeck and P. Zahler, Springer-Verlag, Berlin, Germany, (1981) pp. 13–42.
32. Daussant, J., N.J. Neucere and L.Y. Yatsu, *Plant Physiol. 44*:471 (1969).
33. Neucere, N.J., *Anal. Biochem. 27*:15 (1969).
34. Yatsu, L.Y., T.J. Jacks and T.P. Hensarling, *Plant Physiol. 48*:675 (1971).
35. Altshul, A.M., L.Y. Yatsu, R.L. Ory and E.M. Engleman, *Ann. Rev. Plant Physiol. 17*:113 (1966).
36. Yatsu, L.Y., and T.J. Jacks, *Arch. Biochem. Biophys. 124*:466 (1968).
37. Tolbert, N.E., *Meth. Enzymol. 31*:734 (1974).
38. Beevers, H., and R.W. Breidenbach, *Ibid 31*:565 (1974).
39. Wiskich, J.T., *Biochem. Plants 2*:243 (1980).
40. Hensarling, T.P., L.Y. Yatsu and T.J. Jacks, *J. Am. Oil Chem. Soc. 47*:224 (1970).
41. Martin, S.S., and H.B. Bosmann, *Exp. Cell Res. 55*:59 (1971).
42. Butler, W.L., and J.E. Baker, *Nature 205*:1319 (1965).
43. Harris, C.E., R.D. Kobes, D.C. Teller and W.J. Rutter, *Biochemistry 8*:2442 (1969).
44. Vance, V.B., and A.H.C. Huang, *J. Biol. Chem. 262*:11275 (1987).
45. Yang, S., and R.S. Criddle, *Biochemistry 9*:3063 (1970).
46. Ji, T.H., J.L. Hess and A.A. Benson, *Biochim. Biophys. Acta 150*:676 (1968).
47. Sprott, G.D., K.M. Shaw and K.F. Jarrell, *J. Biol. Chem. 258*:4026 (1983).
48. Henriques, F., and R.B. Park, *Biochim. Biophys. Acta 430*:312 (1976).
49. Qu, R., S. Wang, Y. Lin, V.B. Vance and A.H.C. Huang, *Biochem. J. 235*:57 (1986).
50. Mani, R.S., and S. Zalik, *Biochim. Biophys. Acta 200*:132 (1970).
51. Holowach, L.P., J.F. Thompson and J.T. Madison, *Plant Physiol. 74*:576 (1984).
52. Neucere, N.J., and E.J. Conkerton, *J. Agric. Food Chem. 26*:683 (1978).
53. Youle, R.J., and A.H.C. Huang, *Amer. J. Bot. 68*:44 (1981).
54. Dechary, J.M., G.L. Leonard and S. Corkern, *Lloydia 33*:270 (1970).
55. Jacks, T.J., T.P. Hensarling and L.Y. Yatsu, *Econ. Bot. 26*:135 (1972).
56. Cerff, R., and S.E. Chambers, *J. Biol. Chem. 254*:6094 (1979).
57. Bigelow, C.C., *J. Theoret. Biol. 16*:187 (1967).
58. Barrantes, F.J., *Biochem. Biophys. Res. Commun. 62*:407 (1975).
59. Miyazawa, T., and E.R. Blout, *J. Am. Chem. Soc. 83*:712 (1961).
60. Miyazawa, T., Y. Masuda and K. Fukushima, *J. Polymer Sci.*:S62 (1962).
61. Hoffpauir, C.L., *Agr. Food Chem. 1*:668 (1953).
62. Lin, Y.H., and A.H.C. Huang, *Arch. Biochem. Biophys. 225*:360 (1983).
63. Ory, R.L., L.Y. Yatsu and H.W. Kircher, *Arch. Biochem. Biophys. 264*:225 (1968).
64. Simpson, T.D., and L.K. Nakamura, *J. Am. Oil Chem. Soc. 66*:1093 (1989).
65. Huang, A.H.C., and R.A. Moreau, *Planta 141*:111 (1978).
66. Fernandez, D.E., R. Qu, A.H.C. Huang and L.A. Staehelin, *Plant Physiol. 86*:270 (1988).
67. Moreau, R.A., K.D.F. Liu and A.H.C. Huang, *Plant Physiol. 65*:1176 (1980).
68. Slack, C.R., W.S. Bertaud, B.D. Shaw, R. Holland, J. Browse and H. Wright, *Biochem. J. 190*:551 (1980).
69. Cheeseman, D.F., and J.T. Davies, *Advan. Protein Chem. 9*:439 (1954).
70. Fisher, H.F., *Biochim. Biophys. Acta 109*:544 (1965).
71. Wanner, G., E.L. Vigil and R.R. Theimer, *Planta 156*:314 (1982).
72. Goldberg, D.B., S. Al-Marayati and E. Gonzalez, *Plant Physiol. 68*:280 (1982).
73. Vance, V.B., and A.H.C. Huang, *J. Biol. Chem. 263*:1476 (1988).

[Received October 11, 1989; accepted February 9, 1990]
[J5826]